Fall 12-9-2022

Hydraulic Redistribution Under Saline Conditions

Josh Gottlieb
Portland State University

Hydraulic Redistribution Under Saline Conditions

An Honors Thesis Presented in Partial Fulfillment of
Bachelor's Degree in Civil Engineering

Josh Gottlieb

Department of Civil and Environmental Engineering
Under the supervision of Dr. Samantha Hartzell
Portland State University
December 2022

Abstract

Water scarcity and soil salinity are dual stressors for plants in arid, salt-affected ecosystems. Hydraulic redistribution, a hydraulic adaptation which moves water through plant roots into dry or saline soil regions along potential gradients, aids plant survival in stressful environments. Recent theory regarding hydraulic redistribution proposes limitations on the process within saline soils. This study applies a minimalist resistor-capacitor model of the soil-plant-atmosphere system to the experimental conditions of a 2010 study investigating hydraulic redistribution in a salt affected area. The effectiveness of the model is evaluated, and a sensitivity analysis is conducted to identify key dynamics affecting the moisture redistribution process. The results indicate that a minimalist model faces limitations when testing the theoretical restrictions on redistribution in saline soil, but certain variables, particularly salt accumulation in the plant, can be predicted with reasonable accuracy. Recent studies on the plant represented by the model, *P. lentiscus*, show agreement with the model predictions, indicating that the experimental conditions are well-captured, and that salt accumulation in plant leaves would be unlikely to impede hydraulic redistribution. Discussion on model limitations and the need for greater internal complexity in the plant component is provided to improve future investigations into salinity-based restriction mechanisms on moisture redistribution through plant roots.

Contents

List of Figures

List of Tables

1 Introduction

As global temperatures rise, many plants face increasing water deficits, putting species with adaptive mechanisms of water management at increased advantage over vulnerable species (Adhikari, Hansen, & Rangwala, 2019). In arid climates, hydraulic redistribution (HR) - the transfer of water between regions of soil facilitated by plant roots (Figure 1) - is an important adaptive strategy that can preserve soil moisture, maintain root health, and facilitate efficient nutrient uptake (Neumann & Cardon, 2012; Orellana, Verma, Loheide, & Daly, 2012). Within certain ecosystems, plants with deep tap roots (phreatophytes) survive by accessing groundwater as a supplemental or primary source of moisture. Studies on HR in phreatophytes include evidence of upward redistribution (from deep soil layers to shallow layers) and reverse distribution (from shallow layers to deep layers) (Scott, Cable, & Hultine, 2008) depending on the particular water potential gradient in the system, which can vary with season and precipitation (Prieto, Armas, & Pugnaire, 2012; Yu et al., 2013). The ability to access both a shallow and deep source of water is a significant adaptation, and in certain climates, the portion of plant transpiration sourced by roots below the water table can make up a significant percentage of the overall groundwater budget (Loheide, Butler, & Gorelick, 2005; Orellana et al., 2012).

In addition to water scarcity, soil salinization is a major threat to agriculture and ecosystems in many of these regions, particularly coastal areas facing a rise in sea levels, which drives the extent of inland salt intrusion (Ullah, Bano, & Khan, 2021). Land use and natural resource planning in arid, salt-affected regions requires detailed understanding of hydrologic processes. The projected change to soil salinity in future decades varies across global zones, and many regions which are currently salt-affected are expected to face more severe issues (Hassani, Azapagic, & Shokri, 2021). Halophytes - salt-tolerant plants - are often the dominant species in these climates, with survival mechanisms that allow them to thrive in saline conditions (Perri, Katul, & Molini, 2019). In land surface investigations, for simulations of plant water storage and transpiration, a large source of variance between models is the uncertainty involved in capturing plant hydraulics, particularly root zone dynamics and their effect on soil moisture (Oorschot, Ent, Hrachowitz, & Alessandri, 2021). Thus, understanding the root-facilitated mechanisms controlling water flux in dry, saline climates is important to improve projections of vegetative and soil health in these regions.

There is abundant evidence of hydraulic redistribution along soil moisture gradients in various climatic zones, with roots in wetter regions of soil transferring moisture to drier regions, facilitating easier water uptake for plants. Hydraulic redistribution has also been observed along salt gradients in saline soils, with plant roots transferring moisture from regions with less salinity to regions of greater salinity (Hao et al., 2009). However, the potential for hydraulic redistribution driven by salinity gradients in arid climates is a topic of recent debate. Bazihizina, Veneklaas, Barrett-Lennard, and Colmer (2017) theorized that limitations exist on HR in saline soils based on two primary dynamics. First, plants in saline soils may accumulate salt in the root xylem, creating a highly negative internal water potential zone in the roots near the emission point, preventing water from being released from the roots back into the soil. Second, a similar process may occur in plant

leaves in saline climates, with salt accumulation stifling HR by decreasing leaf water potential, the osmotic effects of the salt overpowering the positive water potential influence of leaf turgor pressure. This magnification of negative leaf water potential could pull internal plant water into the leaves during predawn periods, rather than allowing release into the dry, saline regions of the soil touching the roots. Bazihizina et al. (2017) developed these arguments using empirical data on salt accumulation effects in the literature, and presented an analysis of existing studies on HR in saline soils to highlight the water potential gradients present in the experiments in relation to the direction of HR observed. The study with the most relevant data, (Armas, Padilla, Pugnaire, & Jackson, 2010), was conducted in an environment where the water potential gradient caused by discrepancy in soil moisture between the saturated and vadose zones was stronger than the water potential gradient due to salinity between the zones. Bazihizina et al. (2017) cite this as evidence that salinity variation may be incapable of driving HR, and state that the results bolster other data indicating salt accumulation can cause limitation on HR.

In this study, a resistor-capacitor (RC) model for the soil-plant-atmosphere (SPAC) system was applied to investigate the results of the Armas et al. (2010) study conducted in a coastal dune system in Almeria, Spain, which observed HR facilitated by *P. lentiscus* in a system with non-saline soil moisture in the dry vadose zone, and a brackish saturated zone penetrated by deep tap roots. *P. lentiscus* is both a phreatophyte and halophyte, which utilizes groundwater through its tap roots during the dry season, and relies more heavily on vadose zone water during times of high precipitation. The minimalist RC model, which represents the vadose and saturated soil zones as discrete reservoirs, was calibrated to simulate the Armas et al. (2010) experiment, using estimated values for key environmental parameters following the methods used by Bazihizina et al. (2017) in their analysis. The goal was to evaluate the effectiveness of a minimalist RC model in capturing the dynamics of a saline, preatophytic SPAC system, in particular, determining whether the model could predict the correct direction of HR and the extent of salt intake based on the experimental results. In addition, the aim was to test the limitations proposed by Bazihizina et al. (2017), and identify the components of both the model and the physical plant system which are key to the redistribution process in saline soils.

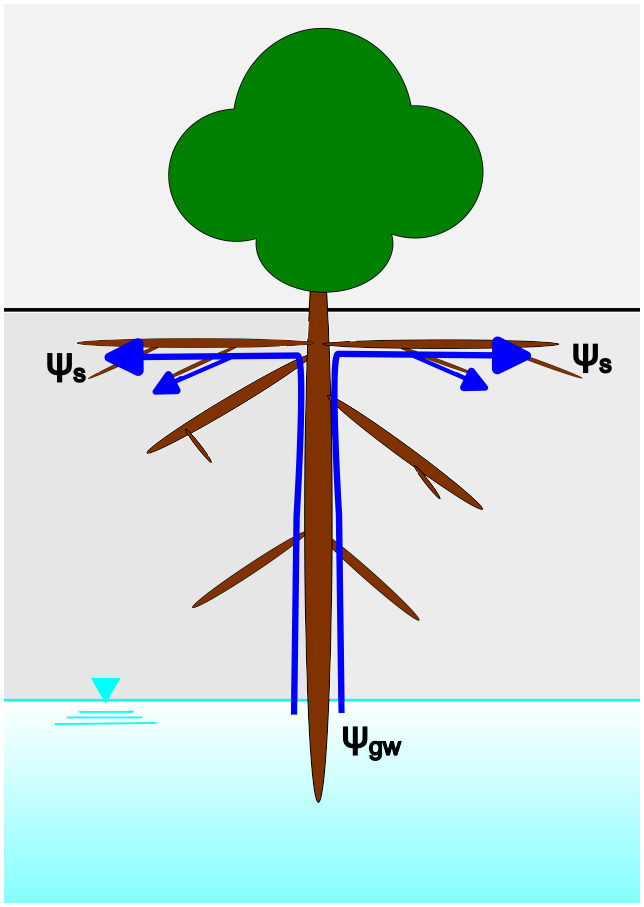

Figure 1: Illustration of hydraulic redistribution (HR). Moisture, s, from the saturated soil zone, Ψ_{gw}, is transported through the plant root system to the drier vadose zone, Ψ_s, when transpiration is low.

2 Methods

2.1 Resistor-Capacitor Model

Resistor-capacitor models for plant hydraulics use a simplified, electrical circuit-style schematic that labels key locations within the plant as nodes, in an analogy to Ohm's law, with pathways between nodes assigned a hydraulic conductance (the inverse of the path's resistance). Hydraulic pathways within the pant with higher conductance facilitate greater water flux, analogous to current, between respective nodes (Tyree, 1997; Li et al., 2021). RC models are useful for understanding general dynamics of the SPAC system with low computational demand, and the ability to capture the effects of the plant's stomatal control on transpiration rates (Daly, Porporato, & Rodriguez-Iturbe, 2004). Previous modeling efforts have incorporated plant water storage into the basic root-to-shoot water pathway in the form of a compartment representing total storage in a specific plant location such as the stem or leaf (Schulte & Nobel, 1989; Bartlett, Vico, & Porporato, 2014; Hartzell, Bartlett, & Porporato, 2018). The RC modelling approach has also been applied to capture salt dynamics

and the varied impacts of salinity on halophytes and glycophytes (Perri et al., 2019).

This minimalist approach was applied to investigate plant dynamics for the Armas et al. (2010) study, with the question of whether an RC model incorporating water storage, salinity, and HR could capture the findings of the experiment. Cáceres et al. (2021) used a similar RC model to investigate water dynamics in a Mediterranean Forest, and their approach informed the construction of the model developed in the present study for a similar climate. The RC model captures many of the same system dynamics as porous media models (Huang et al., 2017), but soil, groundwater, and plant storage components in the RC approach are aggregated into compartments, each assigned a single value of relative moisture and water potential, rather than modeling the SPAC system in many discrete portions using a multitude of compartments.

Dynamic model simulations progress in 30 minute time increments, with soil moisture, hydraulic conductances, water potentials, and salt concentrations updating at each time step. Weather parameters - air temperature, relative humidity, and solar radiation - constrain the variable values at each increment, creating a deterministic progression of system conditions.

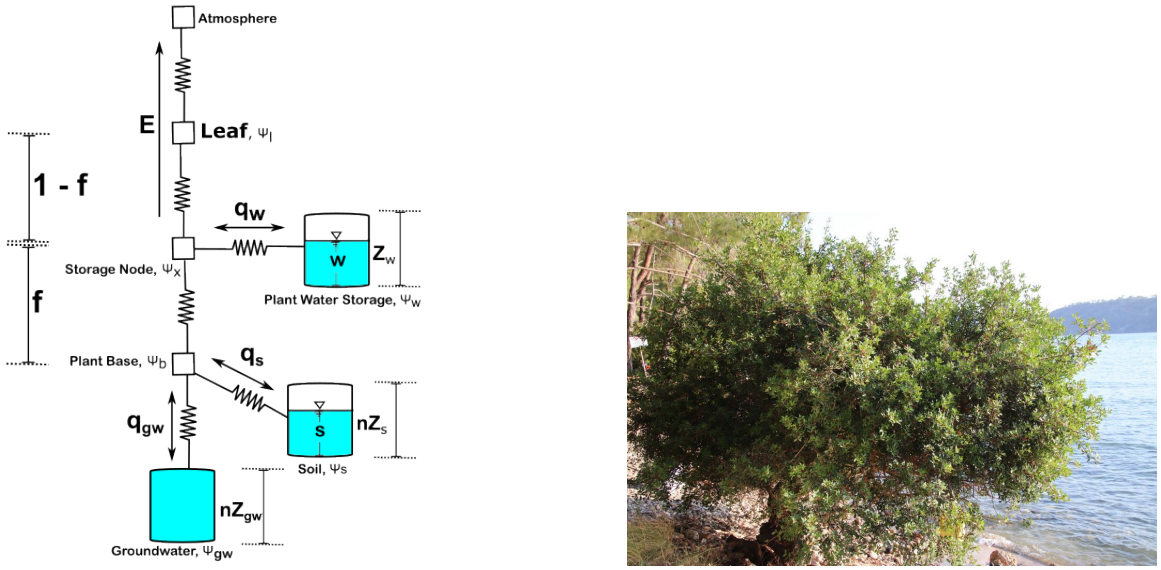

Figure 2: Left: The Soil-Plant-Atmosphere continuum is modeled as a circuit, with water potentials, Ψ, at each node, and resistors between each node. The fluxes from the vadose (soil) and saturated(groundwater) zones to the plant base, q_s and q_{gw} respectively, are positive when entering the plant and negative when exiting via hydraulic redistribution. Right: *P. lentiscus* (Vyatcheslav, 2020).

2.1.1 Water Potentials

Moisture flux within the resistor-capacitor model is driven by differences in water potential between the various nodes of the plant. Water potential, Ψ, is the measure of the potential energy of soil or plant water per unit volume relative to the potential energy of pure water (Koide, Robichaux, Morse, & Smith, 2000). Multiple factors contribute to water potential, and dictate the magnitude

and direction of flow in a system. Cohesion-Tension theory conceptualizes flow through the plant as continuous, with potentials as the forces pulling on unbroken water columns through the plant conduits (Sperry, Adler, Campbell, & Comstock, 1998). Therefore, as long as the water pathway is not broken by cavitation or loss of surface tension, the flow travels from points of high potential (less negative) to points of low potential (more negative). Matric potential, Ψ_m is the component of the total potential created by the intermolecular and surface tension forces of water within soil pores and in plant compartments (Tyree, 2003). As soil dries out, the energy required to extract it increases as adhesive forces become stronger, and matric potential becomes more negative, creating a gradient between dry regions and wetter regions with less negative matric potential. Another source of variability in water potential is salinity, typically measured in terms of the electrical conductivity of the liquid. The potential arising due to the presence of salt ions in soil water is called osmotic potential, and is commonly calculated using Van't Hoff's Law for each ionic species of interest, i.e., (Campbell & Norman, 1998)

$$\Psi_o = -Cv\phi_i RT_w \,, \tag{1}$$

where Ψ_o is osmotic potential, C is the ionic concentration, v is the molecular count of ions per molecule of the compound, ϕ_i is the osmotic coefficient (usually assumed as 1 for solutes in biological systems), R is the universal gas constant, and T_w is the water temperature. Gravity is another source of water potential in plant hydraulic systems, with gravitational potential, Ψ_g, becoming significant in tall plants, such as trees, where the leaf canopy and soil are far apart vertically. The individual components of water potential are summed to determine total potential for various nodes within the RC model, i.e.,

$$\Psi = \Psi_m + \Psi_o + \Psi_g \,. \tag{2}$$

2.1.2 Soil-Root System

The coastal dune system studied in Armas et al. (2010) is made up of sandy soil, with a saline groundwater table 4-5 m below the surface influenced by seawater intrusion, and non-saline soil water in the vadose zone. *P. lentiscus*, the species of interest, has significant salt tolerance, and adapts to the dry coastal ecosystem by expanding a dimorphic root system: a dense layer of lateral roots in the dry upper layers of the vadose zone, and a deep burrowing tap root able to penetrate the saline saturated zone. Tap root systems are known to provide survival advantages for plants in multiple ways, including restoration of vadose zone water through HR and allowing access to an additional water source when dry conditions deplete moisture in the upper soil layers (Orellana et al., 2012). Evidence from numerous studies shows that dimorphic root systems are able to transfer groundwater towards the surface after prolonged drought periods when shallow water is depleted (Armas et al., 2010), and potentially transfer water downwards from the vadose layer when the gradient of moisture is more negative towards the water table (Scott et al., 2008).

In order to capture the effects of the osmotic and matric potential gradients between the dry,

non-saline vadose zone and the saline, saturated soil zone, the RC model separates the two layers into uniform, composite containers, following Vervoort and Zee (2009). Each layer is assigned a relative soil moisture value, s, which is the decimal percentage of soil pore space filled with water (Rodriguez-Iturbe, Porporato, Ridolfi, Isham, & Cox, 1999). The pore space, V_v represents voids in the soil not filled with solid particles: $n = \frac{V_v}{V_{soil}}$, where n, the soil porosity, is the fraction of soil volume made up of pore space.

Volumetric soil water content ($VWC = \frac{\text{Volume water}}{\text{Volume soil}}$), the volume of water per total volume of soil, was calculated using the gravimetric water content ($GWC = \frac{\text{Mass water}}{\text{Mass soil}}$) values measured by Armas et al. (2010) and dividing the masses of water and soil by their densities respectively: $GWC = \frac{\text{kg water}}{\text{kg soil}}$ and $VWC = \frac{\frac{\text{kg water}}{\rho_w}}{\frac{\text{kg soil}}{\rho_{soil}}} = GWC * \frac{\rho_{soil}}{\rho_w}$, where ρ is the density (in $\frac{\text{kg}}{\text{m}^3}$) of each particular substance.

Relative soil moisture is then calculated by dividing the volumetric water content by the porosity, $s = \frac{VWC}{n}$. At saturation, $s = 1$, and the saturated zone soil moisture in the resistor-capacitor model was assumed to be constant throughout the modeling duration, i.e. $s_{gw} = 1$. Groundwater uptake by the tap roots of phreatophytes can often lower the water table significantly, however the tap root's rapid growth rate (up to 13 mm/day in some species) means that over relatively short timespans of 1-4 months it is a reasonable assumption that the roots are in constant contact with saturated soil (Orellana et al., 2012; Gou & Miller, 2014).

The matric potential of soil water (Ψ_m) and soil hydraulic conductivity (K_s) were derived using the Clapp and Hornberger (1978) empirical equations:

$$\Psi_m = \Psi_{m,sat} s^{-b}\,, \tag{3}$$

$$K_s = K_{sat} * s^{2b+3}\,, \tag{4}$$

where the empirical parameters b, $\Psi_{m,sat}$ (matric potential at saturation), and K_{sat} (hydraulic conductivity at saturation) are shown in Table 1 along with other parameters used in the soil-root portion of the model. Soil hydraulic conductivity decreases with declining soil moisture because air enters soil pores, overcoming the surface tension forces of water, similar to cavitation effects in the plant xylem, fracturing the "hydraulic rope", and decreasing the magnitude of water flux from the soil to the plant roots (Sperry et al., 1998). Soil moisture in the vadose zone is updated in the model at time steps of 30 minutes using the mass balance equation:

$$nZ_r \frac{ds}{dt} = q_s - E_v\,, \tag{5}$$

where evaporation, E_v, follows a linear decline from a maximum value, $E_{v_{Max}}$, as the soil moisture approaches the hygroscopic point, s_H,

$$E_v = \begin{cases} E_{v_{Max}}(s - s_H), & s \geq s_H\,, \\ 0, & s < s_H\,, \end{cases} \tag{6}$$

and leakage from the upper soil compartment into the groundwater is assumed to be negligible in the experiment's conditions (Porporato, Laio, Ridolfi, & Rodriguez-Iturbe, 2001).

Root water uptake, q, in the RC model was calculated based on the assumption that the radial conductance of moisture, through the soil and across the permeable barrier at the endodermis of the plant root, was the limiting conductance, rather than the axial conductance of the water along the root's interior length towards the plant stem. This assumption reflects the justification of Huang et al. (2017) that energy lost in the axial conduction of water through the length of a root is often less significant to the dynamics of the overall system than the resistance posed by the hydraulic conductivity loss in the dry soil layers. The radial soil-root conductance was calculated as a series of the soil conductance, k_s, and root permeability, k_r, using the following equation:

$$k_{sr} = \frac{k_s k_r}{k_s + k_r}\,, \tag{7}$$

where k_{sr} is the combined soil-root conductance on a root surface area basis. The value of k_r was set constant (see Table 1) and k_s was calculated using root architecture parameters:

$$\begin{aligned} k_s &= \tfrac{K_s}{l}, \\ l &= \tfrac{0.53}{\sqrt{\pi * B}}\,. \end{aligned} \tag{8}$$

The variable l represents the mean distance that soil moisture has to travel to contact a fine root and B is the root length density - the amount of total combined root length per unit of soil volume (Vogel, Dohnal, Dusek, Votrubova, & Tesar, 2013; Huang et al., 2017). Soil-root conductance, g_{sr}, was converted from the root conductance on a surface area basis to a total value using $g_{sr} = k_{sr} * A_r * Z_r$ where A_r is the root area density ($A_r = 2\pi r_r B$), the area of root exposed per unit soil volume, r_r is the average fine root radius, and Z_r is the root zone depth of the particular soil zone. The root distribution of *P. lentiscus* decreases in fine root area density with depth, and Mattia, Bischetti, and Gentile (2005) reported that a logarithmic decay function fit the decay pattern most accurately. No studies have specifically looked at mature *P. lentiscus* plants with deep tap roots, so a logarithmic profile was used in the sensitivity analysis as a base case, but variation in the root area density distribution was applied to account for the uncertainty in root zone architecture. The root area density value for each soil compartment was determined using the method employed by Vervoort and Zee (2009), taking an integral of the root density decay function over the vertical bounds of each soil zone, and normalizing the integral in each region to a decimal percentage share of the overall root area density, which was then multiplied by the total root area density in the system (Figure 3). The integral bounds were selected using the Armas et al. (2010) profile of soil saturation. Studies on root conductances in dimorphic systems have shown that root conductance for tap roots can be significantly larger than for shallow, lateral roots (Orellana et al., 2012). In the RC model, the dynamic of larger conductance in the deeper tap roots is reflected by the effect of the maximum relative soil moisture in the saturated zone, which raises the value of hydraulic conductivity k_s significantly, increasing water contact with the deep roots, giving rise to

a much higher soil-root conductance than that of the vadose zone root system.

The equation for root uptake from both soil compartments is the following:

$$q = g_{sr} * (\Psi_s - \Psi_b) \tag{9}$$

The difference between the total water potential at the basal node of the plant, Ψ_b, and the potential of soil water, Ψ_s, is thus the main determinant of the magnitude of root update and HR, and the value of this gradient fluctuates with transpiration demand and the accompanying leaf water potentials, Ψ_l, which are driven by atmospheric conditions.

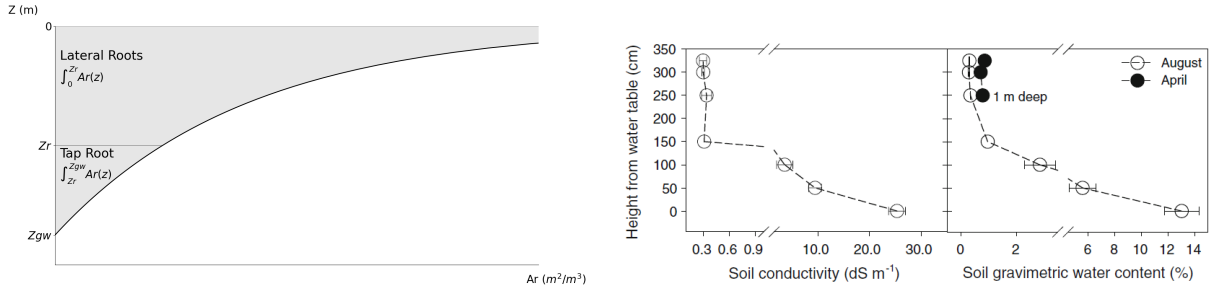

Figure 3: Left: Method for calculating the root area density (A_r) for lateral (vadose zone) and tap roots (saturated zone), following (Orellana et al., 2012). The distribution function, $A_r(z)$ is a logarithmic function for root area density, Z_r is depth of the vadose zone, and Z_{gw} is the total depth to groundwater. Right: The soil profile of soil conductivity and gravimetric water content (GWC) measured by Armas et al. (2010) in the coastal dune system.

HR is driven by heterogeneity in the root zone. The driver of flow directionality, as for the root water uptake, is the potential gradient between the soil compartments and the basal node. HR is represented conceptually in the model as negative root flux, and is reliant on the same root conductances and potential gradients, justified by the passive mechanism of HR (Neumann & Cardon, 2012). Darcian flux, the flux driven by the moisture gradient between soil layers which is not conducted through the rooting system, was considered negligible based on its relatively low magnitude in comparison to root transport. In addition, the decision to divide the soil into two compartments (saturated and vadose zones) in the circuit schematic was made based on a desire to test the minimalist approach for modelling HR, meaning fluid exchange between the two compartments not facilitated by root transport was outside of the scope of study. With the addition of the above ground plant storage compartment, the question of flow direction and magnitude between the groundwater, soil, and plant storage, which all takes place within the conduit system of the plant, resembles a three reservoir problem, common in studies of hydraulics.

Previous SPAC models have calculated the flux of salt mass between soil zones and plant water over multi-year timescales (Runyan & D'Odorico, 2010). For the duration of the Armas et al. (2010) study (4 months), both the volume of water within the compartments and the uptake of salt ions dictate salinity concentration, and consequently osmotic potential (Perri et al., 2019). Salinity in the saturated zone was assumed to be static over the course of simulations due to a

high degree of salt exclusion by the roots (Perri et al., 2019), and the large volume of the saturated zone compared to the small magnitude of salt mass. A simplifying assumption that 100 percent of the salt content was NaCl was made for osmotic potential calculations (Equation 1), as relative magnitude differences in osmotic potential between soil zones was more pertinent to the model results than the ionic varieties present in the system. To allow for salt accumulation in the plant water storage, water uptake through the basal node is assumed to transport salt mass based on the concentration of the source and the filtration efficiency, FE, which represents the percentage of salt prevented from entering the roots. All salt mass entering the plant is then assumed to accumulate in the storage container, adding to the magnitude of storage concentration using the equation:

$$\frac{dC_w}{dt} = \frac{q_s C_s (1 - FE) + q_{gw} C_{gw} (1 - FE)}{w Z_w}, \tag{10}$$

where $\frac{dC_w}{d_t}$ is the flux of the ionic concentration in plant storage water, w is the percentage of available storage volume occupied in the plant, and Z_w is the total available storage volume. Salt was assumed to only enter the plant, with no salt exiting the root with redistributed water, i.e. when when root uptake was negative, salt flux from root to soil was 0. This assumption lead to a higher prediction of plant salt accumulation, which was beneficial for testing the Bazihizina et al. (2017) theory that salt accumulation in plant water storage is a restrictive mechanism on HR.

Table 1: Soil/Root Parameters and Dynamic Variables

	Description	Value	Units
Constant			
$E_{v_{Max}}$	Maximum Evaporation Flux from Soil	3 [b]	mm day^{-1}
k_r	Root Permeability	10^{-8} [d]	s^{-}1
ϕ_i	Osmotic Coefficient of NaCl	1	-
ρ_a	Density of Air	1.27	kg m^{-3}
ρ_w	Density of Water	998	kg m^{-3}
r_r	Radius of Fine Roots	$2 * 10^{-4}$	m
T_w	Water Temperature	293	°C
v	Ionic Count per Molecule NaCl	2	-
Z_r	Depth of Soil Rooting Zone	2 [e]	m
Z_{gw}	Depth to Groundwater Table	3.5 [e]	m
Varied Parameter			
A_r	Root Surface Area Density	Varied	m^2 m^{-3}
b	Soil Curve Constant	Varied [a]	-
B	Root Length Density	Varied	m m^{-3}
FE	Filtration Efficiency	Varied [c]	-
K_{sat}	Saturated Soil Conductivity	Varied [a]	cm day^{-}1
l	Mean path length of soil moisture to fine root surface	Varied	m
n	Soil Porosity	Varied [a]	-
s_H	Hygroscopic point of relative soil moisture	Varied [a]	-
Dynamic Variable			
C_{gw}	Salt Concentration in Groundwater		mol m^{-3}
C_s	Salt Concentration in Soil		mol m^{-3}
$q_{i,j}$	Water Flux From Node i to Node j		μm s^{-1}
E_v	Evaporation Flux from Soil		μm s^{-1}
g_{gwr}	Groundwater-Root Conductance		μm s^{-1} MPa^{-1}
g_{sr}	Soil-Root Conductance		μm s^{-1} MPa^{-1}
GWC	Gravimetric Water Content		-
K_s	Soil Conductivity		cm day^{-}1
k_s	Soil Conductance		s^{-1}
k_{sr}	Soil-Root Conductance on a root area basis		μm s^{-1} MPa^{-1}
Ψ_s	Soil Water Potential		MPa
Ψ_{gw}	Groundwater Potential		MPa
Ψ_b	Basal Node Water Potential		MPa
Ψ_o	Osmotic Potential		MPa
Ψ_m	Matric Potential		MPa
s	Relative Soil Moisture		-
VWC	Volumetric Water Content		m^3 m^{-3}

[a] Values for loamy sand and sand were taken from Rodríguez-Iturbe and Porporato (2005)
[b] Approximation based on reasonable values from Rodríguez-Iturbe and Porporato (2005)
[c] Approximation based on Perri et al. (2019)
[d] Approximation based on Vogel et al. (2013)
[e] (Armas et al., 2010)

2.2 Plant Xylem and Water Storage

The water flow through the above ground portion of the plant is conducted through the plant xylem, represented in the RC model as a conductance pathway spanning the height of the plant, h. Xylem conductance, g_p, decreases with declining leaf water potential due to the cavitation process, whereby the flow of moisture through the xylem conduits breaks down due to embolism formation, which was first modelled by Sperry et al. (1998). Plants have different hydraulic vulnerability curves representing how their xylem conductivity varies with leaf water potential (Sperry et al., 1998). Additionally, different types of plants exhibit different control strategies on water use during drought. Dryland plants tend to be anisohydric, continuing to keep stomata open during periods of high solar radiation, which increases the risk of cavitation, requiring more negative leaf water potentials to overcome decreased conductances to meet transpiration demands (Kannenberg, Novick, & Phillips, 2019). The xylem vulnerability curve for *P. lentiscus* was measured by Vilagrosa, Bellot, Vallejo, and Gil-Pelegrín (2003) as the relationship between leaf-area specific xylem conductivity and leaf water potential, Ψ_l. Plant xylem conductance was calculated from the leaf-specific conductivity (LSC) using $g_p = \frac{LSC(\Psi_l)}{\rho_w h}$, with Ψ_l as the independent variable for the LSC regression equation.

Plant water storage is modeled as a single compartment branching from the transpiration pathway, using a storage conductance, g_w, that regulates the flux between water flowing through the xylem, and water stored in both voids within the xylem (apoplastic storage) and within plant cells (symplastic storage). This type of capacitance has been previously modelled in circuit diagrams, with g_w serving as a representative value for how much water is diverted from the transpiration pathway, ie. the flow from the plant base to the leaves, and retained as internal storage (Schulte & Nobel, 1989; Hartzell, Bartlett, & Porporato, 2017). The exchange between storage and the flow of the transpiration stream is mediated by Ψ_x, a storage node potential located along the path from the basal node to the leaf node. The storage node potential is calculated implicitly when Ψ_l is solved based on atmospheric conditions, and the exchange between plant storage and the transpiration pathway is:

$$q_w = g_w * (\Psi_w - \Psi_x)\,, \tag{11}$$

$$g_w = g_{w_{Max}} * w^d\,, \tag{12}$$

where Ψ_w is the potential of stored plant water, $g_{w_{Max}}$ is the value of the storage conductance at saturation, d is an empirical parameter that reduces the storage conductance as the volume of water in storage decreases, and q_w is the flux out of (positive) or into (negative) the storage compartment.

Storage water potential, Ψ_w, was calculated using the equation for sapwood xylem water potential applied by Chuang, Oren, Bertozzi, Phillips, and Katul (2006) following empirical relationships from Kumagai (2001):

$$w = (\frac{\Psi_{w_0}}{\Psi_{w_0} - \Psi_w})^p\,, \tag{13}$$

where and Ψ_{w_0} and p are empirical constants. The base values of the initial ionic concentration in storage, initial storage volume, and the empirical storage constants were estimated using relative

water content (RWC) and plant sap osmolality data from Armas et al. (2010). Plant water storage concentration was derived from the osmolality measurements, which were converted to osmotic potential using the factor $1\,\frac{\text{mmol}}{\text{kg}} = -2.408\,\text{kPa}$ (Estrada et al., 2021). The influx of salt concentration into the plant water storage during the course of model simulations (Equation 10) was converted to osmotic potential using Van't Hoff's Law (Equation 1), and was added to the baseline plant storage potential (Ψ_w) calculated at each time step using Equation 13. The total water storage capacity Z_w was calculated using the empirical formulas employed by Cáceres et al. (2021) for *P. latifolia*, a salt-tolerant Mediterranean species similar in size and physiology to *P. lentiscus* and commonly growing in similar ecological zones.

The incorporation of a single storage compartment was used for *P.lentiscus*, a softwood tree, because the majority of a tree's water is typically stored in the sapwood of its trunk, and modelling the trunk as a single compartment allowed the minimalist approach to be evaluated (Hartzell et al., 2017). The simplification of treating the stem storage as a single compartment omits the dynamics of internal storage circulation, but the use of the storage container's normalized height variable, f, represents the location of the centroid of water storage volume in the plant system, following the work of Bartlett et al. (2014).

Table 2: Plant Xylem/Water Storage Parameters and Dynamic Variables

	Description	Value	Units
Constant			
d	Water Storage Conductance Reduction Constant	4 [a]	-
f	Normalized Storage Height Fraction	0.5	-
$g_{w_{Max}}$	Maximum Water Storage Conductance	0.002 [a]	μm s^{-1} MPa^{-1}
h	Height of Tree	3.5 [b]	m
p	Plant Water Storage Equation Constant	400 [c]	-
Ψ_{w_0}	Plant Water Storage Equation Constant	3510 [d]	MPa
Z_w	Maximum Depth of Water Stored per Unit Leaf Area	0.012 [e]	m
Dynamic Variable			
C_w	Salt Concentration in Plant Water Storage		mol m^{-3}
g_p	Plant Xylem Conductance on a Leaf Area Basis		μm s^{-1} MPa^{-1}
g_w	Water Storage Conductance		μm s^{-1} MPa^{-1}
LSC	Plant Xylem Conductivity on a Leaf Area Basis		kg m^{-1} s^{-1} MPa^{-1}
Ψ_w	Plant Storage Water Potential		MPa
Ψ_x	Storage Node Water Potential		MPa
w	Relative Water Storage		-

[a] Value estimated based on trials and following Hartzell et al. (2017)
[b] (Armas et al., 2010)
[c] Value taken from Chuang et al. (2006)
[c] Value estimated using data from Armas et al. (2010)
[e] Values from Cáceres et al. (2021) for similar P. Latifolia

2.3 Leaf Level Gas-Exchange

2.3.1 Photosynthesis

Photosynthetic processes were modelled using typical parameters for a C3 plant type, and followed the structure of the Farquhar, von Caemmerer, and Berry (1980) model as employed in the Photo3 system of Hartzell et al. (2017). Net carbon uptake, A_d, was calculated as a product of the carbon demand of the plant, $A_{\phi,c_s,T_l}(\phi, c_s, T_l)$ and a linear reduction function $f_{\Psi_l}(\Psi_l)$, i.e.,

$$A_d = A_{\phi,c_s,T_l}(\phi, c_s, T_l) f_{\Psi_l}(\Psi_l)\,, \tag{14}$$

where ϕ is incoming solar radiation, c_s is the concentration of carbon in the leaf stomata, and T_l is the leaf temperature. The reduction function was assumed to be piecewise, with a linear reduction in A_d between the values of leaf water potential at the onset of water stress and extreme water stress ($\Psi_{l_{A1}}$ and $\Psi_{l_{A0}}$ respectively):

$$f_{\Psi_l} = \begin{cases} 0, & \Psi_l < \Psi_{l_{A0}}, \\ \frac{\Psi_l - \Psi_{l_{A0}}}{\Psi_{l_{A1}} - \Psi_{l_{A0}}}, & \Psi_{l_{A0}} \leq \Psi_l \leq \Psi_{l_{A1}}, \\ 1, & \Psi_l \geq \Psi_{l_{A1}}. \end{cases} \tag{15}$$

Carbon demand was assumed to be a passive diffusion process scaling with stomatal conductance, g_{s,CO_2}, and the gradient of carbon concentration between the leaf stomata (c_s) and the atmosphere (c_a), i.e.,

$$A_{\phi,c_s,T_l}(\phi, c_s, T_l) = g_{s,CO_2}(c_a - c_s)\,. \tag{16}$$

The carbon demand was regulated by either a limitation in Rubisco, the enzyme primarily responsible for carbon fixation, or a limitation of available light (solar radiation) which powers the production of ATP and other necessary molecules in the Calvin Cycle (Zhang & Portis, 1999). Depending on the level of solar radiation, ϕ, leaf temperature, T_l , and stomatal carbon concentration, c_s, the limiting photosynthetic rate, $A_c(c_s, T_l)$ or $A_q(\phi, c_s, T_l)$, which are the Rubisco- and light-limited rate respectively, dictated the unreduced carbon demand:

$$A_{\phi,c_s,T_l}(\phi, c_s, T_l) = \min[A_c(c_s, T_l), A_q(\phi, c_s, T_l)]. \tag{17}$$

$A_c(c_s, T_l)$ and $A_q(\phi, c_s, T_l)$ were calculated using the equations, parameters, and assumptions outlined in Hartzell et al. (2017), with key species specific parameters V_{cmax0} and J_{max0}, the maximum carboxylation rate and maximum electron transport rate, taken from Filella, Llusià, Piñol, and Peñuelas (1998); Correia and Barradas (2000) (see Table 3).

Following Medlyn et al. (2011) and others, the stomatal conductance was scaled inversely with the square root of the atmospheric vapor pressure deficit (VPD), the difference between vapor pressure in the air and the total potential vapor pressure for a given temperature. This emergent relationship was derived from work on stomatal optimization theories (Katul, Palmroth, & Oren,

2009):

$$g_{s,CO_2} = \frac{aA_d}{c_s\sqrt{VPD}}\,, \tag{18}$$

where the parameter a represents the ratio between atmospheric and stomatal carbon concentrations for C3 plants, determined experimentally (Jones, 1992).

2.3.2 Transpiration and Water Balance

The transpiration flux, E, through the leaf stomata and waxy cuticles was determined using the equation:

$$E = g_{sa}\frac{\rho_a}{\rho_w}[SH_l(T_l, \Psi_l) - SH_a]\,, \tag{19}$$

where SH_l and SH_a are the specific humidity in the leaf stomata and the air respectively, and ρ_a and ρ_w are the densities of water and air respectively. The coupled stomatal-atmospheric conductance for water vapor, g_{sa}, is a series conductance of g_s and g_a computed as $g_{sa} = \frac{g_s g_a}{g_s+g_a}$, with g_a, atmospheric conductance, assigned a standard value based on windspeed following Jones (1992). g_s, stomatal conductance to water vapor, was calculated by factoring in the diffusivity ratio of 1.6 between water vapor and CO_2 and adding the cuticular conductance g_{cut}, representing the passive water vapor flux through the waxy cuticles, i.e.,

$$g_s = 1.6g_{s,CO_2} + g_{cut}\,.$$

The atmospherically forced parameters, Ψ_l and T_l, appear in the equations for plant conductance, photosynthesis, and transpiration, and were solved at each time interval of the simulation through use of the water balance and energy balance equations, which, combined with Equation 19, give a unique solution that conforms to environmental conditions. The water balance equation for the RC model relies on the conservation of mass flux through the plant roots, into or out of storage, and exiting the leaf through transpiration. The equations:

$$q_{b,x}(\Psi_b, \Psi_l) = q_{sr}(\Psi_b) + q_{gwr}(\Psi_b)\,, \tag{20}$$

$$q_{b,x}(\Psi_b, \Psi_x) = E - q_w(\Psi_x)\,, \tag{21}$$

$$E = \frac{LAIg_p(\Psi_l)}{1-f}[\Psi_x - \Psi_l]\,, \tag{22}$$

where LAI is the leaf area index (leaf area per unit ground area), state that the flux $q_{b,x}$ from basal node b to storage node x through the plant stem is equal to the transpiration (E) minus the flux into storage (q_w), and transpiration is a function of the potential gradient between storage node x and the leaf node l. These equations allow for the node potentials to be written in terms of leaf water potential as $\Psi_b(\Psi_l)$ and $\Psi_x(\Psi_l)$, and the third equation can be rewritten:

$$E = \frac{LAIg_p(\Psi_l)}{1-f}[\Psi_x(\Psi_l) - \Psi_l]\,. \tag{23}$$

Equation 19 and Equation 23 can be combined with the energy balance equation surface at the leaf surface:

$$\phi = \rho_a c_p [T_l - T_a] + \lambda_w \rho_w E \,, \tag{24}$$

which states that the energy flux of incoming solar radiation, ϕ, is equal to the energy absorbed as specific heat and latent heat fluxes, the two terms on the right side of the equation, where c_p is the specific heat capacity of air, T_a is air temperature, and λ_w is the heat of vaporization of water. Equations 19, 23, and 24 allow the three unknown variables - Ψ_l, T_l, and E - to be solved, with the solution constrained by atmospheric, soil, and water storage variables at each time step.

Table 3: Leaf Photosynthetic and Weather Variables and Parameters

	Description	Value	Units
Parameter			
a	Stomatal Conductance Constant	3.46 [a]	-
c_a	Atmospheric CO_2 concentration	400	ppm
g_a	Atmospheric Conductance	324 [a]	mm s^{-1}
g_{cut}	Cuticular Conductance	0.0249 [b]	mm s^{-1}
J_{max0}	Maximum Electron Transport Rate	60 [c]	μmol m^{-2} s^{-1}
LAI	Leaf Area Index	3 [d]	m^2 m^{-2}
$\Psi_{l_{A0}}$	Maximum Water Stress	-0.3 [e]	MPa
$\Psi_{l_{A1}}$	Onset of Plant Water Stress	-4.55 [e]	MPa
V_{cmax0}	Maximum Carboxylation Rate	37 [f]	μmol m^{-2} s^{-1}
Dynamic Variable			
A_d	Net Carbon Uptake		μmol m^{-2} s^{-1}
A_{ϕ,c_s,T_l}	Carbon Demand		μmol m^{-2} s^{-1}
A_c	Rubisco-Limited Photosynthetic Rate		μmol m^{-2} s^{-1}
A_q	Light-Limited Photosynthetic Rate		μmol m^{-2} s^{-1}
c_s	Stomatal CO_2 concentration		ppm
E	Transpiration		μm s^{-1}
f_{Ψ_l}	Water Stress Reduction Function		-
g_s	Stomatal Conductance to Water		μm s^{-1} MPa^{-1}
g_{s,CO_2}	Stomatal Conductance to CO_2		mol m^{-2} s^{-1}
ϕ	Solar Radiation		W m^{-2}
Ψ_l	Leaf Water Potential		MPa
SH_a	Specific Humidity in Air		kg kg^{-1}
SH_l	Specific Humidity in Leaf		kg kg^{-1}
T_l	Leaf Temperature		°C
VPD	Vapor Pressure Deficit		MPa

[a] (Jones, 1992)
[b] (Bueno, 2021)
[c] (Filella et al., 1998)
[d] (Barradas & Correia, 1999)
[e] (Galmés, Medrano, & Flexas, 2007)
[f] (Correia & Barradas, 2000)

2.4 Sensitivity Analysis

2.4.1 Model Scenario and Calibration

To calibrate uncertain plant parameters, environmental measures taken by Armas et al. (2010) in their HR experiment in the coastal Mediterranean dune were input and the model was run for the length of the experiment. Weather parameters - air temperature, relative humidity, and solar radiation - for Almeria, Spain were retrieved from the the National Solar Radiation Database (NSRDB) for 2017, the data closest in time to the 2008-2009 period of the Armas et al. (2010) study (Sengupta et al., 2018). 2017 was an especially hot year in the region, but solar radiation timing and duration, as well as relative humidity, were taken as reasonable proxies for conditions present during the experiment. The base values for soil moisture and salinity of the soil compartments were set to the values calculated by Bazihizina et al. (2017) from the Armas et al. (2010) study in order to compare the model results to the arguments made in the paper. In the vadose zone, an initial salt mass was calculated based on an initial concentration taken and volume of pore water, both assigned following the analysis of Bazihizina et al. (2017). The concentration is updated at 30 minute time steps based on changes in soil moisture. Values for g_w, d, r_r, Ar at soil surface were calibrated through 3-month simulations using the relative water content (RWC), internal plant salinity, and leaf water potential benchmarks reported by Armas et al. (2010), which were measured during April and August.

2.4.2 Model Trials

To test the relative impact of osmotic and matric potential gradients on the magnitude of HR, 30 day drydown (zero precipitation) trials were conducted. Initial values of soil moisture and salinity concentration were varied in the saturated and vadose zone compartments, to account for heterogeneity in the soil-root system. In addition, root distribution, soil texture, and salt filtration efficiency were changed across trials to clarify relative impacts of plant parameters on HR in comparison to potential gradients, and identify interactions of these factors. Table 4 shows the configuration of these traits, soil moisture, and salinity factors in the trials of the sensitivity analysis. The results of the sensitivity analysis are supplemented by analytical figures, which show the effects of variations of these plant parameters on instantaneous rates of HR during typical predawn conditions.

Table 4: Sensitivity Analysis Trials. Soil moisture (s) was varied in the vadose zone, while soil texture and filtrartion efficiency (FE) was varied in both soil zones. Salinity concentrations (C_{gw}, C_s) and root density ratios ($A_{r_{gw}}$:A_{r_s}) are listed as saturated/vadose zone values respectively. B = base value (90:10), L/H = low/high (85:15), H/L = high/low (95:5).

Trial	s	Salinity Concentrations ($\frac{\text{Mol}}{\text{m}^3}$)	Soil Texture	Root Density Ratio ($A_{r_{gw}}$:A_{r_s})	FE
Base	0.12	300/200	Sand	B/B	0.99
T1	0.12	300/200	Loamy Sand	B/B	0.99
T2	0.09	300/200	Sand	B/B	0.99
T3	0.15	300/200	Sand	B/B	0.99
T4	0.12	300/260	Sand	B/B	0.99
T5	0.12	300/140	Sand	B/B	0.99
T6	0.12	300/200	Sand	L/H	0.99
T7	0.12	300/200	Sand	H/L	0.99
T8	0.12	300/200	Sand	B/B	0.92

3 Results and Discussion

The results of the sensitivity analysis (Figure 4) show the relative impact of important factors on the magnitude of HR in the scenario and conditions of the coastal dune experiment. Of the parameters tested in the analysis, soil moisture and salinity distributions showed the strongest impact on 30-day HR, while root distribution and filtration efficiency, along with other factors including leaf area index and plant water storage parameters had less influence, particularly for the realistic range of values in the experimental system. The magnitude of cumulative HR in the 30 day trials ranged from about 0.1 to 2 mm, with the highest value corresponding to an increase in soil moisture (T3) and the lowest value corresponding to a finer soil texture (T1). The average precipitation during July in Almeria, Spain is approximately 2 mm (AEMET, 2022), which provides context to the potential importance of HR in the region to ecosystem stability, and resistance to desertification, particularly during the dry season.

A clear trend found in the simulations testing the relative importance of the components of the minimalist RC model is that below-ground, root-soil factors seem to play the primary role in determining the potential for HR in a dry, sandy, coastal system with a saline water table, dimorphic roots, and opposite directionality of matric and osmotic potential gradients. Above ground water storage and transpiration-related factors, while relevant to the redistribution of water in the roots zone, exert less of an influence in the minimalist model configuration, and particularly seem to have a muted effect when soil moisture is an obvious limiting factor in root water transport. Conclusions drawn from the relative lack of influence imposed by plant traits on the movement of root water must also be gauged in relation to the limitations of the RC model, and the availability of data provided by the Armas et al. (2010) experiment. However, the model demonstrated the ability to predict the directionality of HR in the system, and performed in fair agreement with measures of plant relative water content and leaf water potential, indicating that a circuit schematic can be used to capture macroscopic dynamics of plant systems in saline soils, and provide a heuristic basis

for questions of HR dynamics.

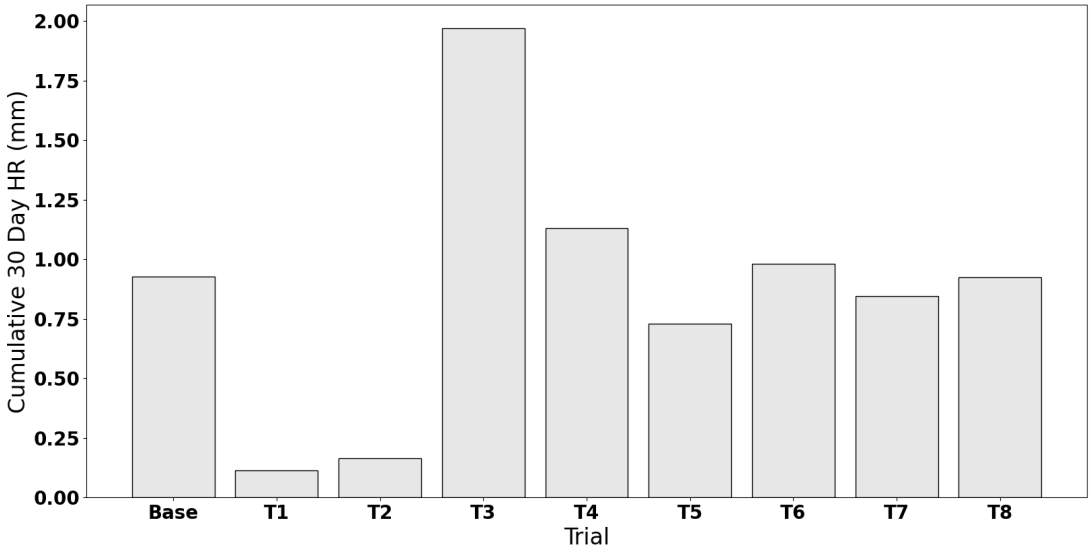

Figure 4: 30 day cumulative hydraulic redistributon (HR) for sensitivity analysis trials

3.1 Influence of Matric and Osmotic Potential Gradients

The influence of water potential gradients between groundwater and soil compartments is the predominant factor determining the magnitude of HR in both saline and non-saline systems, and analysis of the interplay of the components of the potential gradients may be the key to understanding limitations on redistribution. In the context of the schematic proposed by Bazihizina et al. (2017), the experimental conditions of Armas et al. (2010) fall within a type-2 soil environment, with significant contributions of both matric and osmotic potential to the overall potential gradient. An analysis using the base parameters of the experimental setup with a set of typical predawn atmospheric conditions in the model results illustrated that the potential for HR in saline soils, where variation in soil moisture is also a major factor, is best understood by considering the water potential components as connected rather than as distinct drivers of HR.

Figure 5 highlights this intertwined dynamic. It shows that the osmotic water potential gradient causes no significant increase in HR when the matric potential gradient is larger than 1.8 MPa, but has increasing influence as the matric gradient potential decreases. For dryland systems, the osmotic potential gradient's effect is strongly dependent on the soil matric potential gradient, which is developed in conjunction with the hydraulic conductivity of the soil-root system. At levels of soil moisture that optimize soil-root contact and soil hydraulic conductivity, the model results indicate that osmotic potential may be a more potent influence on hydraulic redistribution than matric potential, with heterogeneity of salt in the root zone explaining the majority of HR variation. However, in drier systems, the limiting factor in HR becomes the soil hydraulic conductivity and

the health of drying roots, which diminishes the impact of osmotic gradients on HR. The question of whether there are limitations on HR for plants in saline soils is thus best accompanied by the understanding that there are limitations for HR in soil of any salinity profile that becomes very dry, and this limitation may interact with salinity-specific dynamics to determine the redistribution of soil moisture.

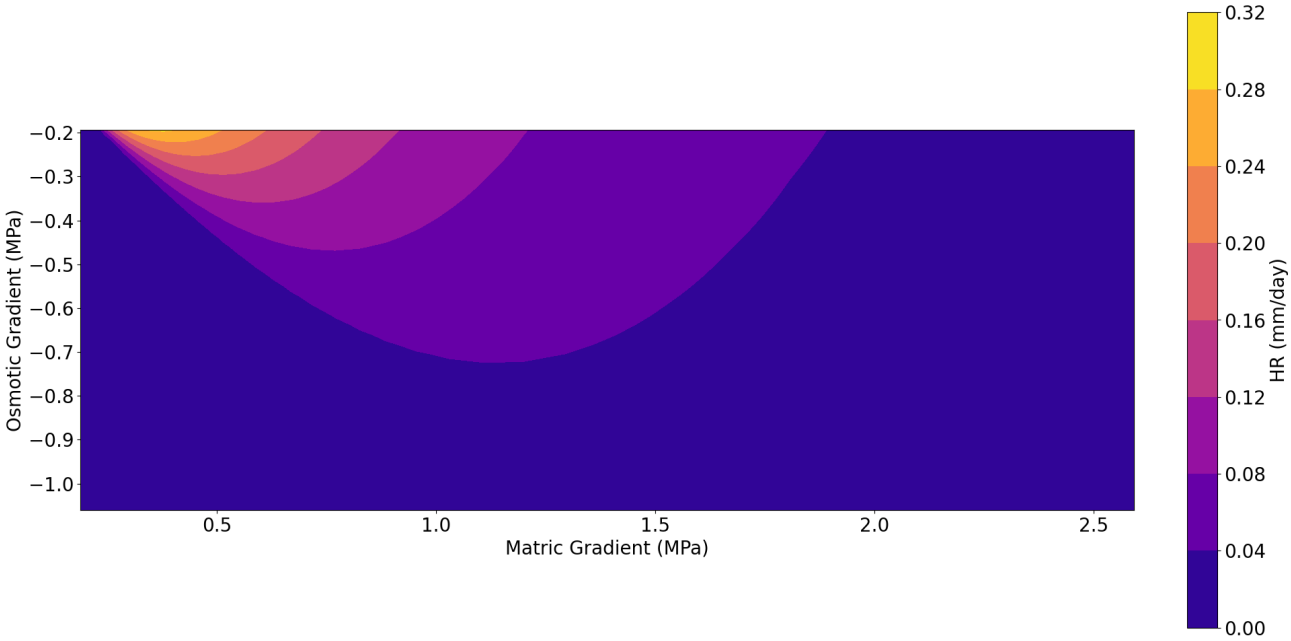

Figure 5: Influence of matric (Ψ_m) and osmotic potential (Ψ_o) gradients on hydraulic redistribution (HR).

3.2 Influence of Soil-Root Conductance

The predominance of osmotic potential as the driver of HR in the coastal dune system occurs when there is a smaller matric potential gradient (≈0.3-0.6 MPa) than the matric gradient present in the experimental conditions. In this smaller matric potential gradient range, the soil is moist enough to facilitate conductance from the root into the soil, while also being dry enough to drive this flux. The great variation in the influence of salinity and osmotic potential relates to the exponential decline of soil hydraulic conductance, and the significance of soil texture on this process. Figure 6 illustrates this pattern in dry, sandy soils, which maintain greater hydrualic conductivity than finer grained soils at low levels of soil moisture. Notably, following the Clapp and Hornberger (1978) equation, which is based on significant empirical evidence, the hydraulic conductivity increases more rapidly at a level of soil moisture near the base level of 0.12 measured by Armas et al. (2010), and the influence of soil texture also increases, as the difference between the two curves at equivalent levels of soil moisture widens.

No soil can be perfectly classified as a sand or loam, and heterogeneity in soil horizons means that different sections of the plant root system will be exposed to soils of slightly differing texture,

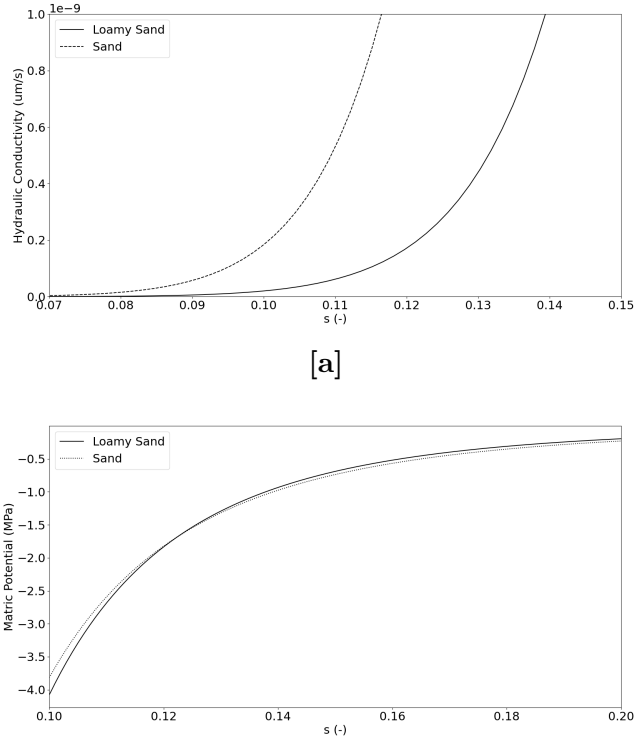

Figure 6: Variation of (a) soil hydraulic conductivity, K_s, and (b) matric water potential, Ψ_m, as a function of soil moisture, s.

with varied ability to conduct moisture to the rootlet surface, as well as away from the root and into the soil during the process of hydraulic redistribution. Variation in soil texture also affects the the magnitude of matric potential that rootlets experience due to the variation in the matric potential-soil moisture curves. The variation in matric potential between sand and loamy sand (Figure 6b) is far less pronounced than the difference in hydraulic conductivity (Figure 6a), however in both soil types, the magnitude of matric potential gets exponentially larger with drydown. Thus, from a root-soil perspective, while the redistributive emission of root water into the surrounding soil is made easier in wetter soil patches with greater hydraulic conductivity, these wetter patches also exert a smaller potential gradient on the root water due to their less negative matric potential. The opposition of these factors and their relative influence on a system's proclivity for HR is understood through the comparison of their governing equations. Equation 3 dictates that matric potential magnitude decreases in conjunction with soil moisture with an exponential factor of b, while soil hydraulic conductance increases with an exponential factor of $2b+3$. Figure 7 captures the effect of these components on HR as soil moisture and texture varies. There is an optimal value of relative soil moisture (near 0.14), for both soil types, at which the gains in conductivity and losses in matric potential magnitude allow for the greatest amount of HR to occur. The fact that sand and loamy sand share an optimal range of soil moisture for HR is due to the similar shape of their hydraulic

conductance and matric potential curves (Figure 6), which is controlled by the empirical constant b in the Clapp and Hornberger (1978) model (Equations 3 and 4). Thus, the magnitude of HR varies greatly between similar soil textures, but the optimal moisture range remains nearly constant. These model results match the conclusions of Bazihizina et al. (2017) on the importance of soil texture and conductivity on hydraulic redistribution, as well as past research results. For example, in an arid Australian system, soil dryness was shown to reduce magnitude of HR without shutting it off completely, partially because of loss of conductivity (Burgess, Pate, Adams, & Dawson, 2000).

The inclusion of salinity as a factor in the model complicates the picture of the role of hydraulic conductivity as a limiting factor of redistribution. Unlike matric potential, which is directly tied to soil moisture, osmotic potential is a function of both salt mass and local soil moisture, both of which can vary greatly, and not necessarily in conjunction, throughout a root zone. The combination of Figures 5 and 7 suggest that osmotic influence influence is greatest when hydraulic conductivity is high, but that the salinity gradient must be stronger in wetter soil patches in order to exert enough pull on root water to extract moisture. In the very dry conditions of the coastal dune system, the salinity gradient is never the primary driver of upward HR due to the highly saline groundwater in the system, which is far saltier than soil water in the upper layers. However, increasing the salt concentration in the vadose zone allows the dryness gradient to be expressed more strongly through an increase in upward HR. In locations with greater moisture conductance and more salt mass, cumulative HR tends to be largest. In summary, from a soil-root perspective, salinity is neither the limiting factor nor the primary driver of redistribution in the dry coastal dune system. However, in wetter patches of the upper root zone, with soil texture more conducive to conducting water, salinity is a major influence on the HR of the system, and this influence may be large enough to provide survival advantage in a Mediterranean climate with minimal precipitation during the dry season. More experimental data for less arid saline climates will help clarify the interaction of osmotic potential and soil hydraulic conductivity, and elucidate whether salt-related limitation on HR exist separate from limitations due to conductivity loss.

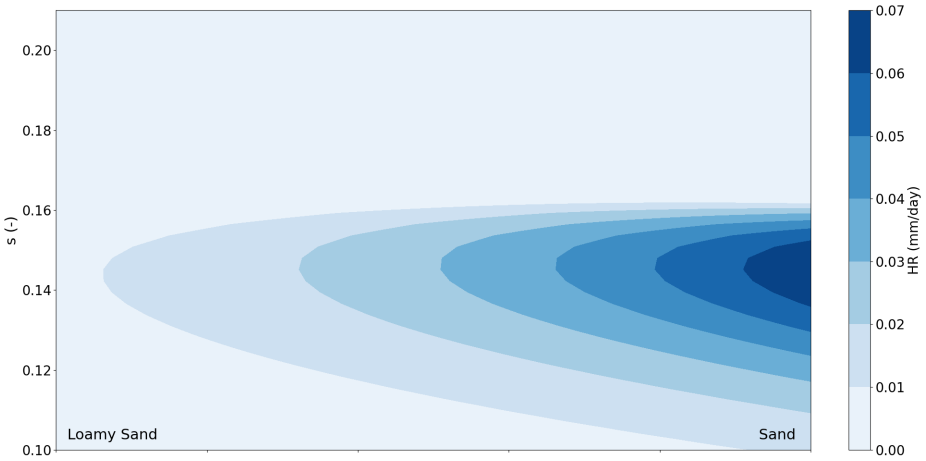

Figure 7: Influence of soil texture on hydraulic redistribution (HR) at varying levels of relative soil moisture, s

3.3 Influence of Root Distribution

Variation of the root area density distribution, particularly the ratio of root area density in the vadose zone to the root area density in the saturated zone, exerted influence on the magnitude of HR in the coastal dune system. Using the assumption of a tapering pattern, as identified by Mattia et al. (2005), with significantly more fine root area in the upper soil than the groundwater layer, the relative ratio of roots within each compartment was shifted to understand the level of impact that each part of the dimorphic system had. Due to the dryness of the upper soil layer, during the drydown trials, the sole source of uptake was through the groundwater roots, with the lateral roots serving only as conduits for redistribution of lifted water and water flowing out of plant storage.

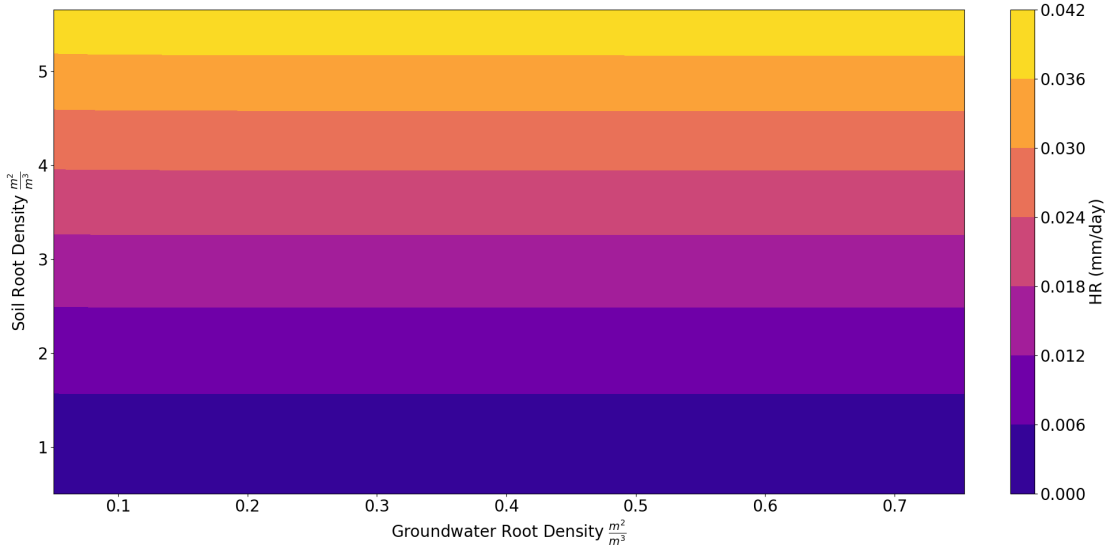

[a]

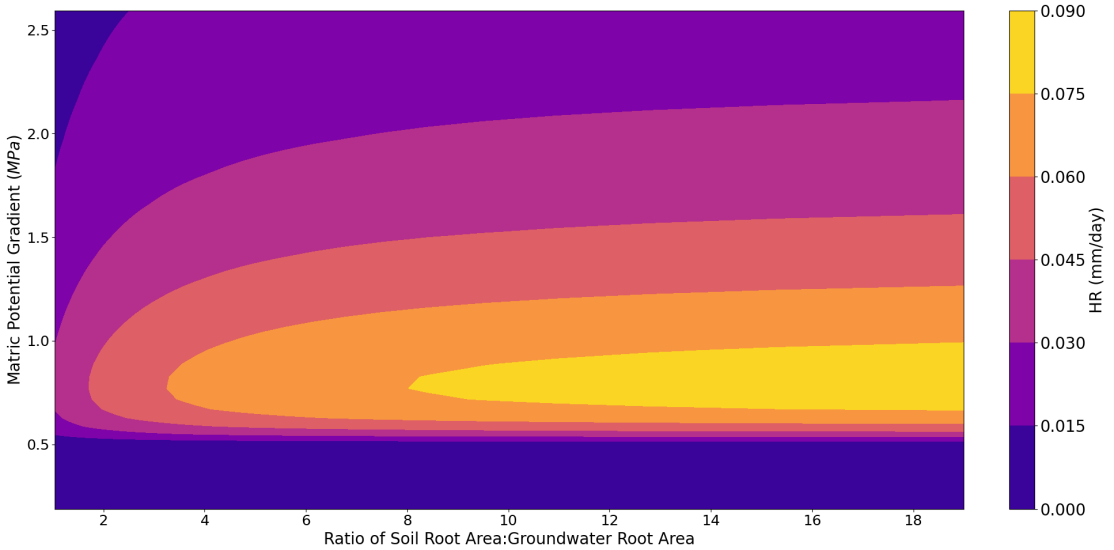

[b]

Figure 8: Influence of root area density (A_r) in the vadose (soil) and saturated (groundwater) zones and matric potential gradient (Ψ_m) on hydraulic redistribution (HR).

Figure 8a highlights the nearly nonexistent influence of groundwater root area density on HR. The clear limiting factor in the coastal dune environment is the root area density of the lateral roots in the vadose zone. Groundwater uptake increases for the plant with a larger spread of groundwater roots, but the previously discussed limitations in soil conductivity prevent prevent an increase in HR without added contact between vadose zone root surface area and soil water. If root surface area is insufficient in dry soil, any additional groundwater uptake tends to contribute to increased transpiration during the day and additional water storage during predawn periods. Figure 8b shows a similar pattern to the soil texture-soil moisture relationship displayed in Figure 7. There is a critical value of of soil moisture and accompanying matric potential for which the root area distribution can be an influential factor on HR ($\Psi_m \approx 0.7 - 0.9$ MPa, $s \approx 0.14 - 0.15$), with decreasing influence outside of these conditions. This is because HR scales linearly with available root surface area in the vadose zone. Outside of the optimal range of soil moisture illustrated in Figures 7 and 8b, the magnitude of HR is so limited by the influence of soil hydraulic conductance and matric potential that the linear amplification of increased root area on HR has a neglible effect.

The 30 day trials conducted in the sensitivity analysis were run assuming a static rooting profile. Research shows that plants expand their root systems dynamically on the time scale of months to years (Schymanski, Sivapalan, Roderick, Beringer, & Hutley, 2008), and can forage to find nutrient and moisture rich patches in soils (Shemesh, Arbiv, Gersani, Ovadia, & Novoplansky, 2010). In addition, expanding the root density in the upper soil layer, while beneficial to soil moisture balance during the dry season, can prove costly to plants when roots in drier regions lose conductivity and function, and require biophysical maintenance. The short-term simulations thus capture the immediate benefits of expanded root density in the dry upper layer, but not the long term factors that may also affect the survival of the plant.

3.4 Salinity in Plant Water Storage

The two primary arguments proposed by Bazihizina et al. (2017) for the existence of limitations on HR in saline soils both relate to the magnitude and interior location of salt uptake within the plant. To attempt to elucidate the process of salt uptake and some of its controlling factors, filtration efficiency - a key trait in most halophytes (Perri et al., 2019) - was varied, and mass transport of salt ions was conjointly allowed to increase. Figure 9 shows the effect filtration efficiency has on the total water potential in plant storage when salt mass is allowed to accumulate. In multiple ways, the RC model likely overestimates the amount that salt accumulation impacts storage potential. First, all salt mass taken in through root water uptake is assumed to accumulate in the storage compartment, making the osmotic potential more negative. In reality, halophytic plants possess multiple methods of osmoregulation - the partial regulation of of osmotic potential - through physiological processes beyond salt filtration (Perri et al., 2019), including accumulation of salt in cell vacuoles, modifications to cellular transporters, and control over ionic distribution (Alvarez, Rodríguez, Broetto, & Sánchez-Blanco, 2018). Second, the 30 day drydown simulations assume no precipitation occurs during the period, while even the small amount of typical precipitation in the

coastal dune system would dilute salinity in the root profile, reducing salt uptake.

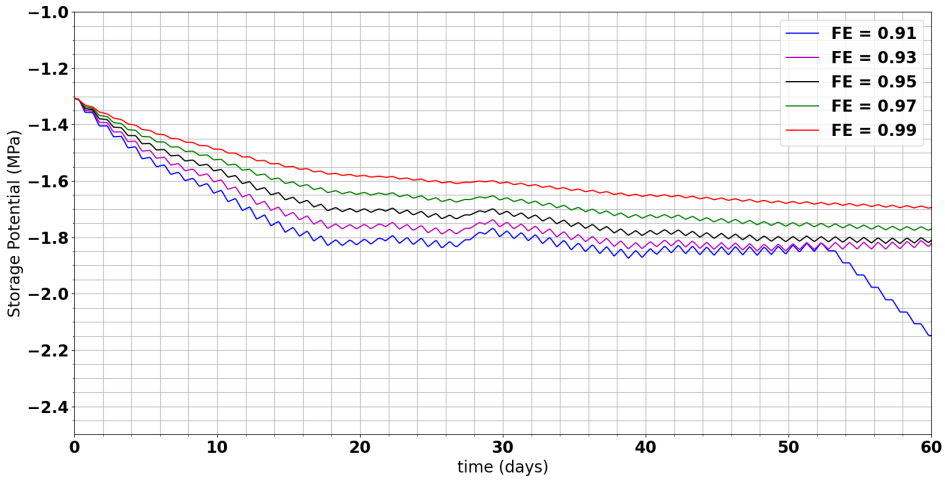

Figure 9: Relationship between filtration efficiency, FE, and plant water storage potential, Ψ_w. For seasonal periods where saline water is the main source of root water uptake, Ψ_w tends to equilibrate when FE is high, but extended reliance on saline water can cause high levels of salt accumulation.

The base value for filtration efficiency, $FE = 0.99$, was determined based on RWC and twig osmolality data reported during the Armas et al. (2010) experiment for April and August within the coastal dune system. The total decrease in relative water content, ΔRWC, over the 4 month period was just 5%, meaning plant water did decline, but that water loss was well controlled, even during the driest months of the year. Greater salt uptake tends to limit plant water storage loss due to the increase in osmotic pull on storage water, meaning lower filtration efficiency serves to prevent water loss significantly. Based on the previously mentioned simplifications - that all salt mass accumulates in water storage during the trial - it is also likely that this osmotic potential driven restriction on water loss is over-predicted. However, the assumption that all salt intake ends up in an internal water storage location that exerts osmotic potential on other compartments within the soil-plant-atmosphere system still provides a reasonable mechanism for analysing the Bazihizina et al. (2017) hypothesis, which was explicitly formulated based on the osmotic potential within the plant.

The results of varying the filtration efficiency in the model indicate that if plant water storage is viewed as a single compartment within *P. lentiscus*, the salt intake during a typical dry period is not enough to make it a dominant sink to the extent that HR is limited. Figure 10 shows that even for a relatively low value of filtration efficiency ($FE = 0.91$), a full month of drydown conditions do not cause the storage water potential to become more negative than the potential of the vadose zone. When the duration of salt uptake with a low FE is extended, however, eventually salt accumulation becomes the dominant influence on storage water potential (Figure 9), with storage volume reaching a level near full capacity. For FE values which accurately represent the water content of the plant

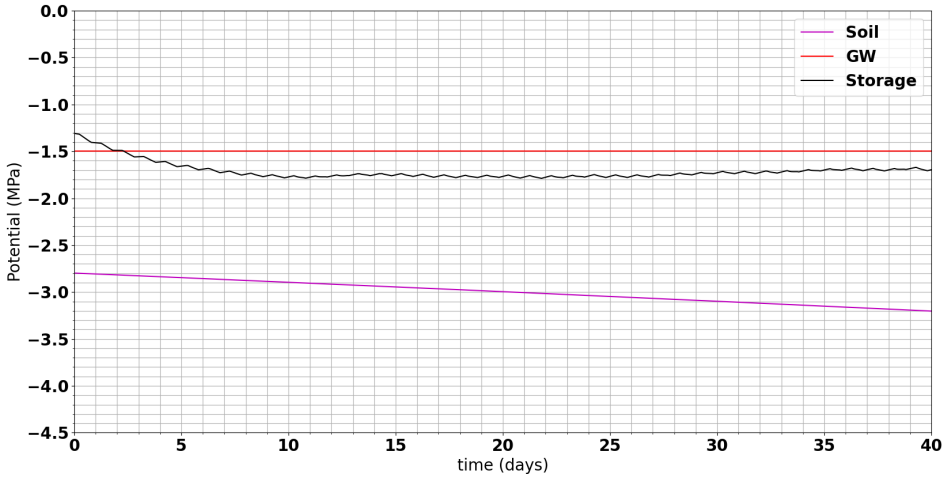

Figure 10: Change in plant water storage potential (Ψ_w) relative to vadose and saturated zone water potentials (Ψ_s, Ψ_{gw}) during an extended simulation with a relatively high level of salt uptake ($FE = 0.91$)

during drydown, the change in storage potential is less pronounced. In the base case ($FE = 0.99$), the potential drop is just 0.2 MPa, from -1.3 to -1.5 MPa, barely below the potential of the saline groundwater, and fitting well with the change in osmolality measured by Armas et al. (2010) during the coastal dune experiment. As Tattini et al. (2006) note based on their study of *P. lentiscus*, a greater fraction of the change in plant water storage osmotic potential tends to come from salt accumulation than change in relative water content. This mechanistic nuance is captured by the RC model, and indicates the high degree of salt filtration that halophytes can develop to, among other survival benefits, retain the capability to redistribute water through their root system without plant water storage acting as a dominant sink during periods of low transpiration. The model also indicates that while halophytes may retain the capacity for HR when using saline water sources seasonally, prolonged dependence on saline water could lead to prohibitive level of accumulation if other osmoregulation mechanisms are not available.

3.5 Model Evaluation and Limitations

There are several important caveats to the conclusions drawn based on the RC model, particularly the osmotic storage component. Namely, certain aspects of the model may reduce its explanatory power for testing the hypothesis of Bazihizina et al. (2017) regarding the potential limitations on HR. The first aspect of the hypothesis, that salt concentration can magnify in the root xylem of plants (particularly during periods of low transpiration) preventing the release of water into the soil, is not well analyzed by the RC model, which collapses all water storage into a single representative compartment. Research by Clipson and Flowers (1987) on root magnification of salt concentration found more than twice the osmotic potential in the root xylem of a halophyte during

low transpiration periods as compared to daytime conditions. The RC model is not able to capture this level of spatial and temporal variation in xylem salinity, and thus cannot definitively provide resolution on this particular limitation. An improved RC model, which incorporates root xylem and leaf storage (Figure 11), could capture the complexity of the internal storage system, and provide the spatial resolution to better investigate the potential sources of HR limitation. Alternatively, a porous media model similar to the scheme developed by Huang et al. (2017) with an incorporation of soil salinity could be used to discretize the root zone, stem, and leaf canopy, helping to complexify internal osmotic and storage gradients.

Even without the incorporation of root and leaf storage, the results of the simplified RC model, in addition to the data provided by Bazihizina et al. (2017) and other studies on *P. lentiscus*, provide evidence that complicates the reasoning laid out in the HR limitation hypothesis. The empirical data from Clipson and Flowers (1987) for halophyte S. maritima do show an increase in xylem ionic concentration during periods of low transpiration, but the ionic concentration appears to plateau at a level below the salinity concentration present in the soil water provided as a source (200 mol/m^3), as this amplifying effect was actually less pronounced in more saline soil (400 mol/m^3). The trials were for 28 days, indicating that salinity uptake in the root zone may initially cause xylem salt concentration to increase, but that some mechanism may limit the upper threshold of this effect, even in more saline soil.

A study on long term salt uptake by *P. lentiscus* conducted by Alvarez et al. (2018) did find significant amplification of the salt concentration in the roots and leaves compared with the stem (1407, 1227, and 503 mMol kg^{-1}) of a plant given saline irrigation, however the measurements did not account for potential compartmentalization of the ions in cell vacuoles. These levels were found after 11 months of saline irrigation, which suggests that salt accumulation could potentially reach concentrations posing a restriction on HR in *P. lentiscus* if the only driving gradient between the root and soil is osmotic, with no additional matric potential gradient, and if the use of saline water is year round, rather than a dry season adaptation, balanced by the use of non-saline soil water during the wet season. Another questionable aspect of the root water concentration limitation proposed by Bazihizina et al. (2017) is whether the accumulation tends to occur only in the parts of the root system where saline water uptake occurs, or whether salts are transported from these predominant uptake zones inside the roots to other regions where where less uptake and more HR would presumably occur, i.e. rootlets in saltier patches of soil where less water is absorbed from the soil.

The second limitation on HR proposed by Bazihizina et al. (2017), that salt accumulation in plant leaves could become a dominant sink during periods of low transpiration, is also not ideally answered using the simplified RC model, which would benefit from an additional water storage compartment for plant leaves. Previous RC model studies have incorporated leaf water storage (Cáceres et al., 2021), and there is greater empirical data on leaf turgor and conductance patterns than is available for stem storage. The data found by Alvarez et al. (2018) suggest that year round irrigation can lead to a significant accumulation of osmotic potential in the plant leaves. Total

leaf storage water potential in *P. lentiscus*, however, was found to equilibrate at -1.71 MPa after 8 weeks of saline treatment under high levels of solar radiation in a separate study, with leaf turgor increasing as ions attracted more water to the symplastic compartments (Tattini et al., 2006). This potential is well above the total potential of the vadose zone in the Armas et al. (2010) study, which would suggest that under dry conditions, or an environment with a very strong salinity gradient, leaf ion accumulation would not prevent HR.

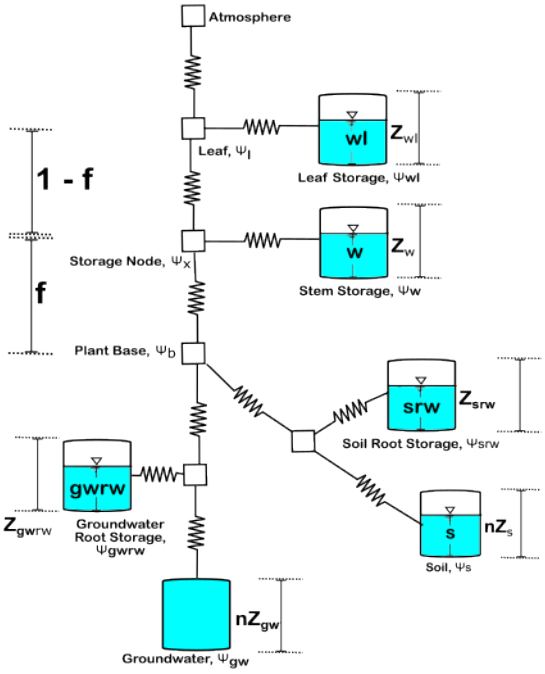

Figure 11: A modified resistor-capacitor (RC) model which could test the limitations on hydraulic redistribution (HR) posed by osmotic potential (Ψ_o) in the root xylem and leaf storage water

Other aspects of the simplified RC model could be added and improved in future investigations to better represent soil-root dynamics. Axial root conductance (friction loss in root xylem) is not considered in the RC model, based on the assumption of radial conductance as the predominant bottleneck in the hydraulic system. Additionally, the xylem vulnerability data for *P. lentiscus* indicates that it is resistant to embolisms, particularly at the levels of leaf water potential reported in the Armas et al. (2010) experiment. However, it is possible that axial root conductance could influence the magnitude of root water redistribution in other ecological settings, as shown in other experiments conducted during dry seasons (Warren, Meinzer, Brooks, Domec, & Coulombe, 2007), and could provide more accuracy in future modeling efforts (Bazihizina et al., 2017). Reduction in axial root conductance due to salinity has also been observed in some previous reports (Bazihizina et al., 2017). Castillo-Campohermoso et al. (2020) showed a reduction in axial root conductance specifically in mastic tree, however, that reduction appeared to level off for soil water salt concentrations above 100 mMol. The influence of soil texture on HR magnitude is also simplified in the RC model, since root-soil contact, the amount of surface area of soil particles touching the root

surface, is not well expressed in the soil-root conductance equation. Figure 7 shows that coarser soil correlates with greater magnitude of HR in the RC model, however, previous experiments provide evidence that coarser soils can sometimes provide less conductivity (Bazihizina et al., 2017; Wang, Tang, Guppy, & Sale, 2009). Without clear data on the distribution of soil heterogeneity in the setting of the Armas et al. (2010), it is hard to say whether the pattern reproduced by the model is accurate (greater conductivity loss in finer soils), and may require refined simulation of the effects of root contact in addition to soil hydraulic conductivity.

4 Conclusion

Hydraulic redistribution is a vital process for plants in arid climates, which often also face challenges from soil salinization. Hypothetical limitations on HR propounded by Bazihizina et al. (2017) were developed based on the lack of strong evidence for redistribution in saline soils, as well as an empirical pattern of salt accumulation in plant roots and leaves which could prevent the emission of root water into surrounding soils. This study evaluated whether a minimalist RC model of the Soil-Plant-Atmosphere continuum could reproduce the results of the most detailed study on HR in a saline climate (Armas et al., 2010), and applied sensitivity analysis to test the influence of various plant parameters on HR. The direction of moisture redistribution, change in plant relative water content, and accumulation of salt in stem water storage was well captured by the simplified RC model, but key complexities - mechanisms of salt incorporation and division of the plant xylem into smaller sections - were highlighted, and should be incorporated into future models to better understand the proposed limitations to HR. Studies on the magnitude and internal location of salt accumulation, specifically in *P. lentiscus* and other halophytes, match the results of the minimalist model, suggesting that in the conditions of the Armas et al. (2010) study salt accumulation would not be large enough to shut down HR, providing a counterexample to the Bazihizina et al. (2017) hypothesis. Future studies should investigate species-specific salt storage mechanisms, implement more spatially discrete mapping of the SPAC system, and model environments where the osmotic gradient is the more dominant factor for HR than the matric gradient. These modifications will be useful in further testing the barriers to HR that may arise in certain saline regions.

References

Adhikari, A., Hansen, A. J., & Rangwala, I. (2019). Ecological water stress under projected climate change across hydroclimate gradients in the north-central united states. *Journal of Applied Meteorology and Climatology*, *58*, 2103-2114. doi: 10.1175/JAMC-D-18-0149.1

Agencia Estatal Meteorology (AEMET). (2022). *Standard climate values.* Retrieved from `https://www.aemet.es/en/serviciosclimaticos/datosclimatologicos/valoresclimatologicos`

Alvarez, S., Rodríguez, P., Broetto, F., & Sánchez-Blanco, M. J. (2018). Long term responses and adaptive strategies of Pistacia lentiscus under moderate and severe deficit irrigation and salinity: Osmotic and elastic adjustment, growth, ion uptake and photosynthetic activity. *Agricultural Water Management*, *202*, 253-262. doi: 10.1016/J.AGWAT.2018.01.006

Armas, C., Padilla, F. M., Pugnaire, F. I., & Jackson, R. B. (2010). Hydraulic lift and tolerance to salinity of semiarid species: Consequences for species interactions. *Oecologia*, *162*, 11-21. doi: 10.1007/s00442-009-1447-1

Barradas, M. C. D., & Correia, O. (1999). Sexual dimorphism, sex ratio and spatial distribution of male and female shrubs in the dioecious species Pistacia lentiscus L. *Folia Geobotanica 1999 34:1*, *34*, 163-174. doi: 10.1007/BF02803082

Bartlett, M. S., Vico, G., & Porporato, A. (2014). Coupled carbon and water fluxes in CAM photosynthesis: modeling quantification of water use efficiency and productivity. *Plant and Soil*, *383*, 111-138. doi: 10.1007/s11104-014-2064-2

Bazihizina, N., Veneklaas, E. J., Barrett-Lennard, E. G., & Colmer, T. D. (2017). Hydraulic redistribution: limitations for plants in saline soils. *Plant Cell and Environment*, *40*, 2437-2446. doi: 10.1111/pce.13020

Bueno, A. B. (2021). *Ecophysiological adaptations of cuticular water permeability of plants to hot arid biomes* (PhD Thesis, Universität Würzburg). doi: 10.25972/OPUS-16783

Burgess, S. S. O., Pate, J. S., Adams, M. A., & Dawson, T. E. (2000). Seasonal water acquisition and redistribution in the australian woody phreatophyte, Banksia prionotes. *Annals of Botany*, *85*, 215-224. doi: 10.1006\anbo.1999.1019

Campbell, G. S., & Norman, J. M. (1998). *An introduction to environmental biophysics.* Springer.

Castillo-Campohermoso, M. A., Broetto, F., Rodríguez-Hernández, A. M., de Abril Alexandra Soriano-Melgar, L., Mounzer, O., & Sánchez-Blanco, M. J. (2020). Plant-available water, stem diameter variations, chlorophyll fluorescence, and ion content in Pistacia lentiscus under salinity stress. *Revista Terra Latinoamericana*, *38*(1), 103. doi: 10.28940/terra.v38i1.510

Chuang, Y. L., Oren, R., Bertozzi, A. L., Phillips, N., & Katul, G. G. (2006, 2). The porous media model for the hydraulic system of a conifer tree: Linking sap flux data to transpiration rate. *Ecological Modelling*, *191*, 447-468. doi: 10.1016/j.ecolmodel.2005.03.027

Clapp, R. B., & Hornberger, G. M. (1978). Empirical equations for some soil hydraulic properties. *Water Resources Research*, *14*(4), 601-604. doi: 10.1029/WR014i004p00601

Clipson, N. J. W., & Flowers, T. J. (1987). Salt tolerance in the halophyte suaeda maritima (l.) dum. the effect of salinity on the concentration of sodium in the xylem. *The New Phytologist*, *105*(3), 359-366. doi: 10.1007/BF00392237

Correia, O., & Barradas, M. C. D. (2000). Ecophysiological differences between male and female plants of Pistacia lentiscus L. *Plant Ecology*, *149*(2), 131-142. doi: 10.1023/A:1026588326204

Cáceres, M. D., Mencuccini, M., Paul, N. M.-S., Limousin, J. M., Coll, L., Poyatos, R., ... Martínez-Vilalta, J. (2021). Unravelling the effect of species mixing on water use and drought stress in mediterranean forests: A modelling approach. *Agricultural and Forest Meteorology*, *296*. doi: 10.1016/j.agrformet.2020.108233

Daly, E., Porporato, A., & Rodriguez-Iturbe, I. (2004). Coupled dynamics of photosynthesis, transpiration, and soil water balance. part I: Upscaling from hourly to daily level. *Journal of Hydrometeorology*, *5*. doi: 10.1175/1525-7541(2004)005⟨0546:CDOPTA⟩2.0.CO;2

Estrada, Y., Fernández-Ojeda, A., Morales, B., Egea-Fernández, J. M., Flores, F. B., Bolarín, M. C., & Egea, I. (2021). Unraveling the strategies used by the underexploited amaranth species to confront salt stress: Similarities and differences with quinoa species. *Frontiers in Plant Science*, *12*. doi: 10.3389/fpls.2021.604481

Farquhar, G. D., von Caemmerer, S., & Berry, J. A. (1980). A biochemical model of photosynthetic CO2 assimilation in leaves of C3 species. *Planta*, *149*, 78-90. doi: 10.1007/BF00386231

Filella, I., Llusià, J., Piñol, J., & Peñuelas, J. (1998). Leaf gas exchange and fluorescence of Phillyrea latifolia, Pistacia lentiscus and Quercus ilex saplings in severe drought and high temperature conditions. *Environmental and Experimental Botany*, *39*, 213-220. doi: 10.1016/S0098-8472(97)00045-2

Galmés, J., Medrano, H., & Flexas, J. (2007). Photosynthetic limitations in response to water stress and recovery in mediterranean plants with different growth forms. *New Phytologist*, *175*(1), 81-93. doi: 10.1111/j.1469-8137.2007.02087.x

Gou, S., & Miller, G. (2014). A groundwater-soil-plant-atmosphere continuum approach for modelling water stress, uptake, and hydraulic redistribution in phreatophytic vegetation. *Ecohydrology*, *7*(3), 1029-1041. doi: 10.1002/eco.1427

Hao, G. Y., Jones, T. J., Luton, C., Zhang, Y. J., Manzane, E., Scholz, F. G., ... Goldstein, G. (2009). Hydraulic redistribution in dwarf rhizophora mangle trees driven by interstitial soil water salinity gradients: Impacts on hydraulic architecture and gas exchange. *Tree Physiology*, *29*, 697-705. doi: 10.1093/treephys/tpp005

Hartzell, S., Bartlett, M. S., & Porporato, A. (2017). The role of plant water storage and hydraulic strategies in relation to soil moisture availability. *Plant and Soil*, *419*, 503-521. doi: 10.1007/s11104-017-3341-7

Hartzell, S., Bartlett, M. S., & Porporato, A. (2018). Unified representation of the C3, C4, and CAM photosynthetic pathways with the photo3 model. *Ecological Modelling*, *384*, 173-187. doi: 10.1016/j.ecolmodel.2018.06.012

Hassani, A., Azapagic, A., & Shokri, N. (2021). Global predictions of primary soil salinization under changing climate in the 21st century. *Nature Communications*, *12*. doi: 10.1038/s41467-021-26907-3

Huang, C. W., Domec, J. C., Ward, E. J., Duman, T., Manoli, G., Parolari, A. J., & Katul, G. G. (2017). The effect of plant water storage on water fluxes within the coupled soil–plant system. *New Phytologist*, *213*. doi: 10.1111/nph.14273

Jones, H. (1992). *Plants and microclimate: A quantitative approach to environmental plant physiology*. Cambridge University Press.

Kannenberg, S. A., Novick, K. A., & Phillips, R. P. (2019). Anisohydric behavior linked to persistent hydraulic damage and delayed drought recovery across seven North American tree species. *New Phytologist*, *222*(4), 1862-1872. doi: 10.1111/nph.15699

Katul, G. G., Palmroth, S., & Oren, R. (2009). Leaf stomatal responses to vapour pressure deficit under current and CO2-enriched atmosphere explained by the economics of gas exchange. *Plant, Cell and Environment*, *32*(8), 968-979. doi: 10.1111/j.1365-3040.2009.01977.x

Koide, R. T., Robichaux, R. H., Morse, S. R., & Smith, C. M. (2000). Plant water status, hydraulic resistance and capacitance. In *Plant physiological ecology* (p. 161-183). Springer Netherlands. doi: 10.1007/978-94-010-9013-1_9

Kumagai, T. (2001). Modeling water transportation and storage in sapwood-model development and validation. *Agricultural and Forest Meteorology*, *109*(2), 105-115. doi: 10.1016/S0168-1923(01)00261-1

Li, L., Yang, Z.-L., Matheny, A. M., Zheng, H., Swenson, S. C., Lawrence, D. M., ... Leung, L. R. (2021). Representation of plant hydraulics in the Noah-MP land surface model: Model development and multiscale evaluation. *Journal of Advances in Modeling Earth Systems*, *13*(4), e2020MS002214. doi: 10.1029/2020MS002214

Loheide, S. P., Butler, J. J., & Gorelick, S. M. (2005). Estimation of groundwater consumption by phreatophytes using diurnal water table fluctuations: A saturated-unsaturated flow assessment. *Water Resources Research*, *41*(7), 1-14. doi: 10.1029/2005WR003942

Mattia, C., Bischetti, G. B., & Gentile, F. (2005). Biotechnical characteristics of root systems of typical mediterranean species. *Plant and Soil*, *278*, 23-32. doi: 10.1007/s11104-005-7930-5

Medlyn, B. E., Duursma, R. A., Eamus, D., Ellsworth, D. S., Barton, V., Crous, K. Y., ... Wingate, L. (2011). Reconciling the optimal and empirical approaches to modelling to stomatal conductance. *Global Change Biology*, *17*(6), 2134-2144. doi: 10.1111/j.1365-2486.2010.02375.x

Neumann, R. B., & Cardon, Z. G. (2012). The magnitude of hydraulic redistribution by plant roots: a review and synthesis of empirical and modeling studies. *New Phytologist*, *194*(2), 337-352. doi: 10.1111/J.1469-8137.2012.04088.X

Oorschot, F. V., Ent, R. J. V. D., Hrachowitz, M., & Alessandri, A. (2021). Climate-controlled root zone parameters show potential to improve water flux simulations by land surface models. *Earth System Dynamics*, *12*(2), 725-743. doi: 10.5194/esd-12-725-2021

Orellana, F., Verma, P., Loheide, S. P., & Daly, E. (2012). Monitoring and modeling water-vegetation interactions in groundwater-dependent ecosystems. *Reviews of Geophysics*, *50*(3). doi: 10.1029/2011RG000383

Perri, S., Katul, G. G., & Molini, A. (2019). Xylem–phloem hydraulic coupling explains multiple osmoregulatory responses to salt stress. *New Phytologist*, *224*(2), 644-662. doi: 10.1111/nph.16072

Porporato, A., Laio, F., Ridolfi, L., & Rodriguez-Iturbe, I. (2001). Plants in water-controlled ecosystems: active role in hydrologic processes and response to water stress: III. vegetation water stress. *Advances in Water Resources*, *24*(7), 725-744. doi: 10.1016/S0309-1708(01)00006-9

Prieto, I., Armas, C., & Pugnaire, F. I. (2012). Water release through plant roots: new insights into its consequences at the plant and ecosystem level. *New Phytologist*, *193*(4), 830-841. doi: 10.1111/j.1469-8137.2011.04039.x

Rodriguez-Iturbe, I., Porporato, A., Ridolfi, L., Isham, V., & Cox, D. R. (1999). Probabilistic modelling of water balance at a point: The role of climate, soil and vegetation. *Proceedings of the Royal Society A*, *455*, 3789-3805. doi: 10.1098/rspa.1999.0477

Rodríguez-Iturbe, I., & Porporato, A. (2005). *Ecohydrology of water-controlled ecosystems: Soil moisture and plant dynamics*. Cambridge University Press.

Runyan, C. W., & D'Odorico, P. (2010). Ecohydrological feedbacks between salt accumulation and vegetation dynamics: Role of vegetation-groundwater interactions. *Water Resources Research*, *46*(11). doi: 10.1029/2010WR009464

Schulte, P. J., & Nobel, P. S. (1989). Responses of a CAM plant to drought and rainfall: Capacitance and osmotic pressure influences on water movement. *Journal of Experimental*

Botany, *40*(1), 61-70. doi: 10.1093/jxb/40.1.61

Schymanski, S. J., Sivapalan, M., Roderick, M. L., Beringer, J., & Hutley, L. B. (2008). An optimality-based model of the coupled soil moisture and root dynamics. *Hydrology and Earth System Sciences*, *12*(3), 913-932. doi: 10.5194/HESS-12-913-2008

Scott, R. L., Cable, W. L., & Hultine, K. R. (2008). The ecohydrologic significance of hydraulic redistribution in a semiarid savanna. *Water Resources Research*, *44*(2). doi: 10.1029/2007WR006149

Sengupta, M., Xie, Y., Lopez, A., Habte, A., Maclaurin, G., & Shelby, J. (2018). The national solar radiation data base (NSRDB). *Renewable and Sustainable Energy Reviews*, *89*, 51-60. doi: 10.1016/J.RSER.2018.03.003

Shemesh, H., Arbiv, A., Gersani, M., Ovadia, O., & Novoplansky, A. (2010). The effects of nutrient dynamics on root patch choice. *PLoS ONE*, *5*(5). doi: 10.1371/journal.pone.0010824

Sperry, J. S., Adler, F. R., Campbell, G. S., & Comstock, J. P. (1998). Limitation of plant water use by rhizosphere and xylem conductance: results from a model. *Plant, Cell & Environment*, *21*(4), 347-359. doi: 10.1046/j.1365-3040.1998.00287.x

Tattini, M., Remorini, D., Pinelli, P., Agati, G., Saracini, E., Traversi, M. L., & Massai, R. (2006). Morpho-anatomical, physiological and biochemical adjustments in response to root zone salinity stress and high solar radiation in two Mediterranean evergreen shrubs, Myrtus communis and Pistacia lentiscus. *New Phytologist*, *170*(4), 779-794. doi: 10.1111/j.1469-8137.2006.01723.x

Tyree, M. T. (1997). The cohesion-tension theory of sap ascent: Current controversies. *Journal of Experimental Botany*, *48*(10), 1753–1765. doi: 10.1093/jexbot/48.315.1753

Tyree, M. T. (2003). Matric potential. *Encyclopedia of Water Science*, 615-617.

Ullah, A., Bano, A., & Khan, N. (2021). Climate change and salinity effects on crops and chemical communication between plants and plant growth-promoting microorganisms under stress. *Frontiers in Sustainable Food Systems*, *5*. doi: 10.3389/fsufs.2021.618092

Vervoort, R. W., & Zee, S. E. V. D. (2009). Stochastic soil water dynamics of phreatophyte vegetation with dimorphic root systems. *Water Resources Research*, *45*(10). doi: 10.1029/2008WR007245

Vilagrosa, A., Bellot, J., Vallejo, V. R., & Gil-Pelegrín, E. (2003). Cavitation, stomatal conductance, and leaf dieback in seedlings of two co-occurring Mediterranean shrubs during an intense drought. *Journal of Experimental Botany*, *54*, 2015-2024. doi: 10.1093/jxb/erg221

Vogel, T., Dohnal, M., Dusek, J., Votrubova, J., & Tesar, M. (2013). Macroscopic modeling of plant water uptake in a forest stand involving root-mediated soil water redistribution. *Vadose Zone Journal*, *12*(1). doi: 10.2136/vzj2012.0154

Vyatcheslav, V. (2020). *Pistacia lentiscus.* Ukrainian Biodiversity Information Network. Retrieved from `https://ukrbin.com/show_image.php?imageid=176533`

Wang, X., Tang, C., Guppy, C. N., & Sale, P. W. (2009, 1). The role of hydraulic lift and subsoil P placement in P uptake of cotton (Gossypium hirsutum L.). *Plant and Soil*, *325*(1), 263-275. doi: 10.1007/S11104-009-9977-1/FIGURES/6

Warren, J. M., Meinzer, F. C., Brooks, J. R., Domec, J.-C., & Coulombe, R. (2007). Hydraulic redistribution of soil water in two old-growth coniferous forests: quantifying patterns and controls. *New Phytologist*, *173*(4), 753-765. doi: https://doi.org/10.1111/j.1469-8137.2006.01963.x

Yu, T., Feng, Q., Si, J., Xi, H., Li, Z., & Chen, A. (2013). Hydraulic redistribution of soil water by roots of two desert riparian phreatophytes in northwest China's extremely arid region.

Plant and Soil, *372*, 297-308. doi: 10.1007/s11104-013-1727-8

Zhang, N., & Portis, A. R. (1999). Mechanism of light regulation of rubisco: A specific role for the larger Rubisco activase isoform involving reductive activation by thioredoxin-f. *Plant Biology*, *96*(16), 9438-9443. doi: 10.1073/pnas.96.16.943